Preparation, Reactions, and Nuclear Magnetic Resonance Spectra of Disubstituted Derivatives of the Octahydrotriborate(1−) Ion, $[B_3H_6XX']^-$ (X = Cl, X' = Cl, NCS, $NCBH_3$, or $NCBH_2Cl$); Molecular Structure of $[B_3H_6Cl_2]^-$ and Partial Structure of $[B_3H_6Cl(NCS)]^-$ †

Marisa Arunchaiya and John H. Morris *
Department of Pure and Applied Chemistry, University of Strathclyde, Glasgow G1 1XL
Steven J. Andrews, Dorothy A. Welch, and Alan J. Welch
Department of Chemistry, University of Edinburgh, Edinburgh EH9 3JJ

The preparation of disubstituted derivatives of $[B_3H_8]^-$ with halogen or pseudo-halogen is reported. Ions studied include $[B_3H_6Cl_2]^-$ (1), $[B_3H_6Cl(NCS)]^-$ (2), $[B_3H_6Cl(NCBH_3)]^-$, and $[B_3H_6Cl(NCBH_2Cl)]^-$. N.m.r. parameters show that the ions are fluxional in solution, and ^{11}B–^{11}B coupling is poorly resolved. The thermal stabilities, and chemical and electrochemical behaviour of representative compounds are described. The molecular structures, illustrated by $[B_3H_6Cl_2]^-$ and $[B_3H_6Cl(NCS)]^-$ relate to that of $[B_3H_8]^-$ with *trans* substituents. Four molecules of $[N(PPh_3)_2][B_3H_6Cl_2]$ crystallise in space group $P2_1/c$ with a = 10.9552(14), b = 12.840(9), c = 24.236(5) Å, and β = 92.298(13)°. R = 0.0728 for 3 267 data measured at room temperature. The $[B_3H_6Cl_2]^-$ ion has effective C_2 symmetry and markedly asymmetric H bridges. $[N(PPh_3)_2][B_3H_6Cl(NCS)]$ crystallises from CH_2Cl_2 as a 1 : 1 solvate with Z = 2 in space group $P\bar{1}$, with a = 11.2855(22), b = 14.4000(21), c = 15.708(4) Å, α = 120.680(17), β = 109.760(18), and γ = 65.971(14)° at 185 ± 1 K. An approximate structure solution affords R = 0.1922 for 5 706 diffraction data.

As part of our investigations into the effects of substitution on the properties of the octahydrotriborate(1−) anion, we now report the preparation, structure, and properties of disubstituted derivatives. Previously, these were known only as by-products in the preparation of monosubstituted species,[1] and no systematic study of their properties has been reported. Interest in the field stems from a number of factors. Since a variety of structures have been observed in the crystallographic investigations of monosubstituted $[B_3H_7X]^-$ (X = H, NCO, NCS, or NCSe) derivatives,[2] and substituted $[B_3H_7X]^-$ (X = Cl or Br) ions have been used to synthesize higher boranes through a route involving thermal decomposition,[3] the structures and thermal stabilities of the disubstituted derivatives are therefore important. A cyanide-substituted borane anion is an intermediate in the synthesis of monocarbon carbaboranes;[4] it is possible that other CN derivatives could also serve as precursors to other carbaborane species. The substituent in monosubstituted $[B_3H_7X]^-$ ions markedly affects the chemical and electrochemical properties of the anion, in particular the oxidation potentials and mechanism of electrochemical oxidation.[5] Details of the n.m.r. spectra of monosubstituted derivatives are governed by fluxional behaviour and partial quadrupolar relaxation.[6] The behaviour and parameters of the disubstituted derivatives are therefore likely to be particularly significant.

Experimental

Starting Materials and Reagents.—The preparations of the $[N(PPh_3)_2]^+$ salts of $[B_3H_7(NCS)]^-$ and $[B_3H_7(NCBH_3)]^-$ were carried out as previously described.[1] Solvents CH_2Cl_2 and CH_3CN were of high-performance liquid chromatography grade, and were dried over CaH_2. The supporting electrolyte, $[NBu^n_4][BF_4]$, was used as supplied by Fluka A.G. 1,3-Dioxolane was dried over Na and distilled before use.

Electrochemical Methods.—Cyclic and a.c. voltammetry were carried out using a model 363, E. G. and G. Princeton Applied Research potentiostat, a Hi-Tek Instruments Ltd. wave-form generator (model PPR1), and home constructed a.c. generator, phase sensitive detector, and amplifier systems. Voltammograms were recorded on a Bryans 25000 *X–Y* recorder. Coulometry was carried out using a Hi-Tek Instruments Ltd. DT 2101 potentiostat, and gated digital integrator. Undivided cells were used for voltammetry, but two-compartment cells separated by Nafion 427 ion-exchange membrane were used for coulometry. Platinum wire or foil working and secondary electrodes were used for most of the work. The reference electrodes were Ag–$AgNO_3$ (0.1 mol dm^{-3}) in CH_3CN but Ag–$[N(PPh_3)_2]Cl$ (0.1 mol dm^{-3}) in dioxolane and PhCN; the reference solution was separated from the anode by a porous ceramic sinter.

N.M.R. Spectra.—These were recorded on Bruker WH250 and WH360 spectrometers (^1H, 250 and 360 MHz; ^{11}B, 80.2 and 115.5 MHz). Chemical shifts are quoted as being negative to high field of the reference standard (BF_3·OEt_2 for ^{11}B and $SiMe_4$ for ^1H). Line shapes were simulated using the U.E.A.-N.M.R. BASIC program. Spectra were normally recorded in deuteriochloroform.

Thermal Measurements.—Thermogravimetric analysis was carried out on a Stanton Redcroft T.G.-150 Thermal Balance. Heating was carried out under an atmosphere of dry nitrogen and in the temperature range 0—400 °C. Differential scanning calorimetry (d.s.c.) was carried out on a Du Pont Instruments 910 Differential Scanning Calorimeter and 990 Thermal Analyzer.

Preparations and Reactions.—(*a*) $[B_3H_6Cl_2]^-$ (1). In a 250-

† *trans*-1,2-Dichloro-1,3;2,3-di-μ-hydro-tetrahydrotriborate(1−) and *trans*-2-chlorohexahydro-1-isothiocyanatotriborate(1−) respectively.

Supplementary data available (No. SUP 23995, 66 pp.): phenyl H-atom co-ordinates, thermal parameters, phenyl ring packing data, view of crystal packing, and structure factors for both compounds; parameters for extended Hückel calculations of $[B_3H_6Cl_2]^-$. See Instructions for Authors, *J. Chem. Soc., Dalton Trans.*, 1984, Issue 1, pp. xvii—xix.

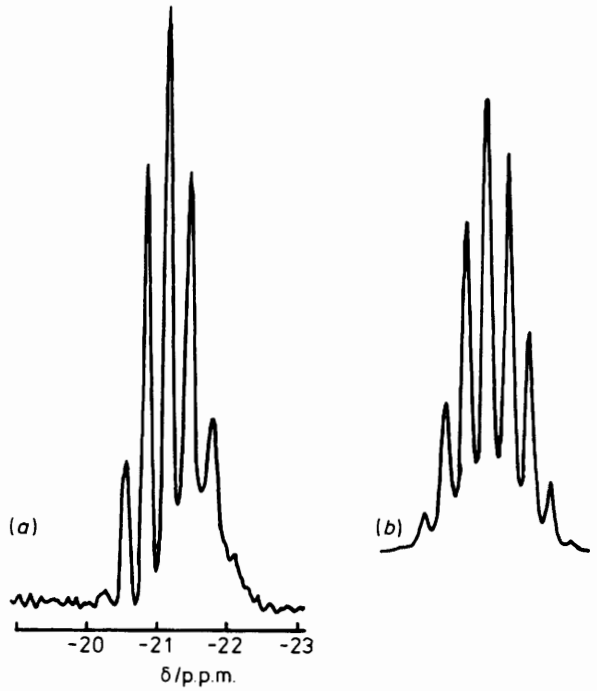

Figure 1. (*a*) ^{11}B N.m.r. (298 K) and (*b*) simulated ^{11}B spectrum of $[B_3H_7(NCO)]^-$

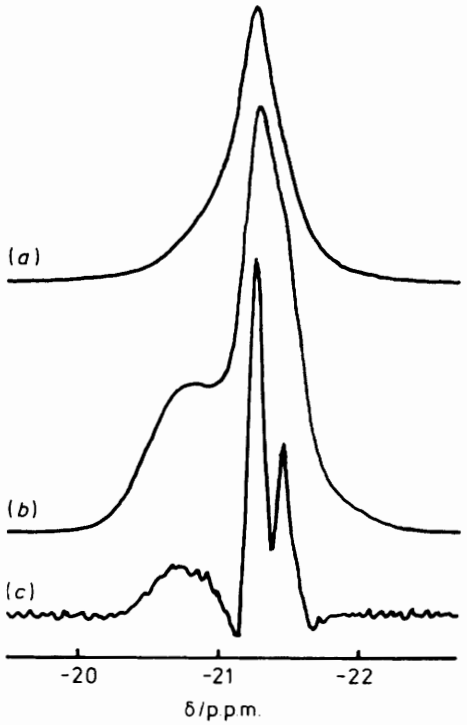

Figure 2. 115.5-MHz ^{11}B-{^1H} N.m.r. spectra of $[B_3H_7(NCO)]^-$ in $CDCl_3$: (*a*) at 303 K, (*b*) at 323 K, and (*c*) line narrowed at 323 K

cm^3 flask fitted with a stop-cock adaptor was placed $[N(PPh_3)_2][B_3H_8]$ (1.4 g, 2.5 mmol) and dried, degassed CH_2Cl_2 (20 cm^3) was condensed in under vacuum. Gaseous HCl (5 mmol) was introduced, and the mixture stirred for 30 min until hydrogen evolution ceased. Solvent was removed under vacuum, and the dry solid was recrystallized from CH_2Cl_2–hexane mixtures to give colourless crystals, identical to those prepared earlier.[1]

(*b*) $[B_3H_6Cl(NCS)]^-$ (2). In a similar manner, $[N(PPh_3)_2][B_3H_7(NCS)]$ (0.318 g, 0.5 mmol) was treated with two successive aliquots (0.5 mmol) of HCl. The *product*, recrystallized from CH_2Cl_2–hexane, gave colourless crystals (Found: C, 65.2; H, 5.2; Cl, 5.2; N, 3.9; S, 4.8. $C_{37}H_{36}B_3ClN_2P_2S$ requires C, 66.3; H, 5.4; Cl, 5.3; N, 4.2; S, 4.8%). The analytical data were obtained after the crystals had been pumped under high vacuum to remove dichloromethane from the solvate. Crystals for *X*-ray diffraction contained 1 mol of CH_2Cl_2 per mol of (2).

(*c*) *Reactions of* $[B_3H_7(NCBH_3)]^-$ *with* HCl. A series of reactions of $[N(PPh_3)_2][B_3H_7(NCBH_3)]$ (0.5 mmol) with HCl (0.5, 1.0, 1.5, 2.0, and 2.5 mmol) was carried out as described in (*a*); solvent was removed, and the products were monitored by ^{11}B n.m.r. spectroscopy. As the HCl ratio was increased, the yield of unreacted $[B_3H_7(NCBH_3)]^-$ decreased, while there was a progressive build-up in the yields of $[B_3H_7(NCBH_2Cl)]^-$, $[B_3H_6Cl(NCBH_3)]^-$, and $[B_3H_6Cl(NCBH_2Cl)]^-$.

(*d*) *Preparation and reactions of* $[B_3H_7(NCO)]^-$. A mixture of $[N(PPh_3)_2][B_3H_8]$ (2.32 g, 4.0 mmol) and Hg_2Cl_2 (0.94 g, 2.0 mmol) was stirred in degassed CH_2Cl_2 (20 cm^3) for *ca.* 1 h until hydrogen evolution ceased. The resulting solution of $[B_3H_7Cl]^-$ was filtered onto $[N(PPh_3)_2][NCO]$ (2.32 g, 4.0 mmol), stirred for 4 h, and the solvent removed under vacuum. The white product was purified by chromatography over silica gel (200 g) which had been treated with hexamethyldisilazane (16 cm^3 in hexane). The eluting solvent was CH_2Cl_2. The yield of *colourless crystals* was 0.23 g, 10% (Found: C, 71.1; H, 6.0; N, 4.4. $C_{37}H_{37}B_3N_2OP_2$ requires C, 71.7; H, 6.0; N, 4.5%). The ^{11}B n.m.r. spectrum [Figure 1(*a*)] comprised a complex multiplet resulting from second-order ^{11}B–^{11}B coupling, and ^{11}B–^1H coupling to seven fluxional hydrogens perturbed by partial quadrupolar relaxation. A spectrum simulated on the basis of the parameter $J(B–H) = 35.0$ Hz, and a chemical shift difference B(1) — B(2)[B(3)] of 35.0 Hz is shown [Figure 1(*b*)]. The ^{11}B-{^1H} n.m.r. spectrum (Figure 2), recorded at 303 and 323 K, also displayed a pattern consistent with a second-order AB_2 system derived from ^{11}B–^{11}B coupling perturbed by partial quadrupolar relaxation.

Reactions of $[N(PPh_3)_2][B_3H_7(NCO)]$ with HCl were carried out as in (*a*), and the products monitored by t.l.c. and ^{11}B n.m.r. The chromatograms indicated at least three components, and the ^{11}B spectra showed resonances at −7.4, −8.8, and −14.0 p.p.m. in an intensity ratio of 1 : 1 : 1, and a number of other sets of resonances (−9.5, −32.0, −11.8, and −20.0 p.p.m.) whose relative intensities varied with experimental conditions. The average shift of the main component (−10.1 p.p.m.) and the similarity of the spectrum to those of $[B_3H_6Cl(NCS)]^-$ and $[B_3H_6Cl(NCBH_3)]^-$ indicate a disubstituted derivative, $[B_3H_6Cl(NCO)]^-$.

A mixture of $[N(PPh_3)_2][B_3H_7(NCO)]$ (0.124 g, 0.2 mmol) with Hg_2Cl_2 (0.047 g, 0.1 mmol) in CH_2Cl_2 (10 cm^3) was stirred for 6 h, after which time the droplets of mercury were filtered from the solution. The solvent was removed under vacuum, and the solid products monitored by ^{11}B n.m.r. The main component was again $[B_3H_6Cl(NCO)]^-$ by analogy with the HCl reaction.

(*e*) *Preparation and reactions of* $[Ag\{B_3H_7(NC)\}_2]^-$. By a method similar to (*d*), $[N(PPh_3)_2][B_3H_8]$ (2.30 g, 4.0 mmol) was treated with Hg_2Cl_2 (0.94 g, 2.0 mmol) and the resulting solution filtered onto Ag(CN) (0.54 g, 4.0 mmol). The product was purified by chromatography on silica gel, using CH_2Cl_2–CH_3CN (25 : 1), and recrystallized from CH_2Cl_2–hexane. The *colourless crystals* deposited silver on prolonged standing, and

decomposed more rapidly in solution (Found: C, 58.8; H, 5.7; N, 5.1. $C_{38}H_{44}AgB_6N_3P_2$ requires C, 58.7; H, 5.7; N, 5.4%).

(*f*) *Substitution reactions on* $[B_3H_6Cl_2]^-$ (1) *and* $[B_3H_6Cl(NCS)]^-$ (2). $[N(PPh_3)_2][B_3H_6Cl_2]$ (2.5 mmol) was freshly prepared from $[B_3H_8]^-$ as in (*a*), and an equimolar quantity of the ligand anions $[BH_3(CN)]^-$, $[NCS]^-$, or $[CN]^-$ were added as $[N(PPh_3)_2]^+$ or Ag^+ salts to the dry solid. CH_2Cl_2 (20 cm^3) was condensed in, and the mixture stirred for 4—5 h. The ^{11}B n.m.r. spectra of the crude products showed only half of the $[B_3H_6Cl_2]^-$ to have reacted, and only one chlorine was substituted. The products were purified by chromatography on treated silica gel as in (*d*). The reaction with $[BH_3(CN)]^-$ led to $[B_3H_6Cl(NCBH_3)]^-$ and $[B_3H_7(NCBH_3)]^-$; that with Ag(CN) gave a product whose ^{11}B spectrum and properties were consistent with $[Ag\{B_3H_6Cl(CN)\}_2]^-$. Substitution reactions on $[B_3H_6Cl(NCS)]^-$ led to products which were identified by ^{11}B n.m.r. spectroscopy as unchanged starting materials and small quantities of unidentified decomposition products. Similar results were obtained with $[B_3H_6Cl_2]^-$ and $[NCO]^-$.

Crystal Structure Determinations.—Suitable crystals of *trans*-$[N(PPh_3)_2][B_3H_6Cl_2$-1,2] (1) and of the dichloromethane solvate of *trans*-$[N(PPh_3)_2][B_3H_6Cl(NCS)$-1,2] (2) were obtained as described above. Crystal structure analyses of both species followed similar procedures, and are therefore described for (1) only, with data in parentheses representing differences in respect of (2)·CH_2Cl_2.

A single crystal, *ca.* 0.5 × 0.5 × 0.1 mm (0.5 × 0.5 × 0.5 mm) was secured to a thin glass fibre (secured inside a subsequently sealed 0.05-cm Lindemann tube under dry nitrogen) with an epoxy resin adhesive. After preliminary photographic screening the crystal was transferred to an Enraf-Nonius CAD4 diffractometer operating with graphite-monochromated Mo-K_α *X*-radiation with $\lambda_{\alpha1} = 0.709\,26$ and $\lambda_{\alpha2} = 0.713\,54$ Å. For (2)·CH_2Cl_2 only, the crystal was slowly cooled to *ca.* 185 K in a stream of cold nitrogen.

Accurate unit-cell parameters were obtained from the least-squares refinement of 25 strong general reflections in the range $14.0 < \theta < 14.5$ (15.0)°. Three-dimensional intensity data were recorded, by ω—2θ scans in 96 steps, in the range $1.0 \leqslant \theta \leqslant 25(27)°$, ω scan widths being computed by 0.85 + 0.35 tanθ. After rapid prescan only those reflections considered significantly intense $\{I \geqslant 0.5\sigma(I)$ [$1.0\sigma(I)$]} were rescanned such that their final net intensity had $I > 33\sigma(I)$, subject to a maximum measuring time of 70 s (60).

Two orientation and two intensity control reflections were remonitored once every 200 reflections and 3 600 s respectively, but subsequent analysis of their net intensities as individual functions of time yielded no detectable crystal movement or decay, or source variation, over the *ca.* 135 (134) h of *X*-ray exposure.

Of 5 972 (8 582) unique reflections corrected for Lorentz and polarisation effects, but not for *X*-ray absorption, 3 267 (5 706) with $F \geqslant 2.0\sigma(F)$ were retained for structure solution and refinement.

Crystal data for (1). $[C_{36}H_{30}NP_2][H_6B_3Cl_2]$, M = 647.6, monoclinic, a = 10.9552(14), b = 12.840(9), c = 24.236(5) Å, β = 92.298(13)°, U = 3 406.3 Å^3 at 290 ± 2 K, Z = 4, D_c = 1.263 g cm^{-3}, $F(000)$ = 1 352, μ(Mo-K_α) = 2.7 cm^{-1}, space group $P2_1/c$ (C_{2h}^5, no. 14) from systematic absences.

Crystal data for (2)·CH_2Cl_2. $[C_{36}H_{30}NP_2][CH_6B_3ClNS]\cdot CH_2Cl_2$, M = 755.1, triclinic, a = 11.2855(22), b = 14.4000(21), c = 15.708(4) Å, α = 120.680(17), β = 109.760(18), γ = 65.971(14)°, U = 1 977.4 Å^3 at 185 ± 1 K, Z = 2, D_c = 1.268 g cm^{-3}, $F(000)$ = 784, μ(Mo-K_α) = 3.5 cm^{-1}, space group $P\bar{1}$ (C_i^1, no. 2) from *E*-statistics and successful refinement.

Both structures were solved by automatic centrosymmetric direct methods [7] followed by an iterative combination of refinement and difference-Fourier syntheses, and were refined by full-matrix least squares. Phenyl groups were treated as rigid, planar hexagons with C–C 1.395, C–H 1.08 Å, U_H* 0.10 (0.05) Å^2, and variable and individual thermal parameters for carbon.

For (1) structure factors were weighted according to $w^{-1} = [\sigma^2(F) + 0.000\,933(F)^2]$, a scheme that afforded no unusual or systematic variation of the root mean-square deviation of a reflection of unit weight *versus* parity group, $(\sin\theta)/\lambda$, F_o, h, k, or l. All non-H atoms were allowed anisotropic thermal motion, and borane H atoms, located from difference-Fourier syntheses, were only positionally refined (U = 0.10 Å^2).

[For (2)·CH_2Cl_2 the refinement would not proceed below its current high R value, and refinement of a weighting coefficient yielded no improvemen . The C and S atoms of the isothiocyanate function are disordered over two sets of positions, with populations of 0.581 and 0.419 calculated from relative peak heights in a ΔF synthesis. Only P, N, S, and borane-Cl atoms were refined anisotropically, and no solvent H atoms were included.]

Refinement converged at R 0.0728, R' 0.0664 (R 0.1922) with a data-to-variable ratio better than 9.5 (34.0) : 1, and the maximum shift-to-error ratio in the final least-squares cycle was <0.1. In a final ΔF synthesis the maximum peak was 0.37 (3.06) e Å^{-3} and the minimum trough −0.45 (−1.73) e Å^{-3} [for (2)·CH_2Cl_2 these could not be chemically interpreted]. Coefficients for analytical approximations to the atomic scattering factors were taken from ref. 8. Tables 1 and 2 list the derived fractional co-ordinates of refined atoms in (1) and (2)·CH_2Cl_2 respectively. Structure solution and refinement employed programs of the SHELX 76 crystallographic package [7] implemented on the University of Edinburgh ICL2972 computer. Molecular geometry calculations were made with XANADU [9] and *X*-RAY 76,[10] and Figures were constructed using ORTEP-II.[11]

Results and Discussion

Preparation and Reactions.—(*i*) *Chlorinations with* HCl. $[B_3H_6Cl_2]^-$ was prepared as its $[N(PPh_3)_2]^+$ salt by treating the corresponding salt of $[B_3H_8]^-$ with HCl, according to equation (i). $[B_3H_6Cl(NCS)]^-$ was similarly obtained from $[B_3H_7(NCS)]^-$ and HCl as in equation (ii), and each of these

$$[B_3H_8]^- + 2HCl \longrightarrow [B_3H_6Cl_2]^- + 2H_2 \quad \text{(i)}$$

$$[B_3H_7(NCS)]^- + HCl \xrightarrow{CH_2Cl_2} [B_3H_6Cl(NCS)]^- + H_2 \quad \text{(ii)}$$

reactions gave the desired product 'cleanly'. In contrast, although $[B_3H_7(NCBH_3)]^-$ also reacted with HCl to produce the disubstituted derivative $[B_3H_6Cl(NCBH_3)]^-$, the reaction was less clean and other products were also obtained.

A series of reactions of $[B_3H_7(NCBH_3)]^-$ with HCl at different molar ratios yielded products in proportions which were dependent on the experimental conditions; from comparisons of these reaction mixtures with others obtained from substitution reactions involving $[B_3H_6Cl_2]^-$ and $[BH_3(CN)]^-$ in which similar species were obtained, we were able to identify the products as $[B_3H_7(NCBH_2Cl)]^-$ and $[B_3H_6Cl(NCBH_3)]^-$ together with traces of $[B_3H_6Cl(NCBH_2Cl)]^-$.

When $[B_3H_7(NCO)]^-$ was treated with HCl, the reaction gave a mixture of products, the major component of which

* The isotropic thermal parameter is defined as $\exp[-8\pi^2U(\sin^2\theta)/\lambda^2]$.

Table 1. Fractional atomic co-ordinates of refined atoms for $[B_3H_6Cl_2]^-$ (1), with e.s.d.s in parentheses *

Atom	*x*	*y*	*z*
P(1)	0.002 26(13)	0.308 18(12)	0.336 57(6)
P(2)	0.247 53(13)	0.315 41(12)	0.289 91(6)
N(1)	0.1096(4)	0.3432(3)	0.298 83(18)
C(12)	−0.2283(4)	0.2235(3)	0.316 52(12)
C(13)	−0.3221	0.1812	0.282 92
C(14)	−0.3082	0.1725	0.226 14
C(15)	−0.2005	0.2060	0.202 97
C(16)	−0.1067	0.2483	0.236 57
C(11)	−0.1206	0.2570	0.293 35
C(22)	−0.0367(3)	0.5181(3)	0.349 44(13)
C(23)	−0.0849	0.6060	0.374 50
C(24)	−0.1517	0.5953	0.421 99
C(25)	−0.1702	0.4967	0.444 41
C(26)	−0.1219	0.4089	0.419 35
C(21)	−0.0552	0.4196	0.371 86
C(32)	0.0926(4)	0.2379(3)	0.438 04(16)
C(33)	0.1298	0.1607	0.475 58
C(34)	0.1159	0.0559	0.461 52
C(35)	0.0649	0.0283	0.409 92
C(36)	0.0277	0.1055	0.372 38
C(31)	0.0415	0.2103	0.386 45
C(42)	0.3046(3)	0.4538(3)	0.374 21(16)
C(43)	0.3837	0.5159	0.406 58
C(44)	0.5069	0.5223	0.394 52
C(45)	0.5511	0.4667	0.350 09
C(46)	0.4720	0.4046	0.317 72
C(41)	0.3488	0.3982	0.329 78
C(52)	0.3552(4)	0.1577(3)	0.353 79(14)
C(53)	0.3799	0.0537	0.366 57
C(54)	0.3374	−0.0250	0.331 10
C(55)	0.2702	0.0003	0.282 85
C(56)	0.2455	0.1043	0.270 06
C(51)	0.2880	0.1830	0.305 53
C(62)	0.3671(3)	0.2776(3)	0.192 66(15)
C(63)	0.3944	0.2999	0.138 19
C(64)	0.3331	0.3801	0.109 85
C(65)	0.2445	0.4380	0.135 98
C(66)	0.2171	0.4157	0.190 45
C(61)	0.2785	0.3355	0.218 79
B(1)	0.6832(9)	0.2903(7)	0.0371(4)
B(2)	0.5949(8)	0.2330(7)	−0.0195(4)
B(3)	0.6582(12)	0.3586(9)	−0.0250(5)
Cl(1)	0.840 15(18)	0.239 00(19)	0.047 10(8)
Cl(2)	0.428 96(19)	0.223 78(18)	−0.007 81(8)
H(13′)	0.692(7)	0.368(6)	0.037(3)
HB(11)	0.622(7)	0.261(5)	0.072(3)
HB(21)	0.636(7)	0.158(6)	−0.021(3)
HB(31)	0.610(7)	0.424(6)	−0.040(3)
HB(32)	0.755(7)	0.382(6)	−0.048(3)
H(23′)	0.610(7)	0.276(6)	−0.062(3)

* Phenyl rings are numbered in a cyclic manner, with C(*i*1) (*i* = 1—3) bonded to P(1) and C(*j*1) (*j* = 4—6) bonded to P(2).

Table 2. Fractional atomic co-ordinates of refined atoms for $[B_3H_6Cl(NCS)]^-\cdot CH_2Cl_2$ with e.s.d.s in parentheses [a]

Atom	*x*	*y*	*z*
P(1)	−0.0676(3)	0.645 07(24)	0.763 01(21)
P(2)	0.1579(3)	0.463 46(25)	0.797 90(22)
N(1)	0.0789(9)	0.5818(8)	0.7954(7)
C(12)	−0.0955(8)	0.7334(6)	0.9601(6)
C(13)	−0.1628	0.8043	1.0415
C(14)	−0.2883	0.8768	1.0296
C(15)	−0.3465	0.8783	0.9364
C(16)	−0.2792	0.8073	0.8551
C(11)	−0.1537	0.7349	0.8669
C(22)	0.0391(7)	0.7782(6)	0.7526(5)
C(23)	0.0423	0.8490	0.7179
C(24)	−0.0589	0.873 5	0.6449
C(25)	−0.1634	0.8273	0.6065
C(26)	−0.1667	0.7565	0.6412
C(21)	−0.0654	0.7320	0.7143
C(32)	−0.1054(9)	0.4851(8)	0.5781(7)
C(33)	−0.1645	0.4061	0.4957
C(34)	−0.2777	0.3940	0.5014
C(35)	−0.3318	0.4608	0.5895
C(36)	−0.2726	0.5398	0.6718
C(31)	−0.1594	0.5520	0.6661
C(42)	0.2813(6)	0.4346(5)	0.6582(5)
C(43)	0.3755	0.3774	0.5954
C(44)	0.463 6	0.273 4	0.5895
C(45)	0.4575	0.2267	0.6464
C(46)	0.3633	0.2840	0.7091
C(41)	0.2752	0.3879	0.7150
C(52)	0.0498(7)	0.2843(6)	0.6713(5)
C(53)	−0.0357	0.2229	0.6460
C(54)	−0.1120	0.2529	0.7148
C(55)	−0.1028	0.3442	0.8088
C(56)	−0.0173	0.4055	0.8341
C(51)	0.0590	0.3755	0.7653
C(62)	0.2908(7)	0.4017(5)	0.9547(5)
C(63)	0.3707	0.4171	1.0479
C(64)	0.4115	0.5143	1.1068
C(65)	0.3725	0.5963	1.0724
C(66)	0.2926	0.5810	0.9791
C(61)	0.2518	0.4837	0.9203
B(1)	0.4120(23)	0.8927(20)	0.6745(18)
B(2)	0.260(3)	0.938(3)	0.598(3)
B(3)	0.257(3)	0.985(3)	0.6994(24)
Cl(1)	0.2623(7)	0.9828(5)	0.5148(4)
N(2)	0.4061(12)	0.8231(11)	0.7156(10)
C(1) [b]	0.4078(23)	0.7520(21)	0.7252(19)
C(2) [c]	0.395(3)	0.8007(24)	0.7789(22)
S(1) [b]	0.4110(7)	0.6560(8)	0.7518(7)
S(2) [c]	0.3795(10)	0.7526(12)	0.8494(11)
C(3)	0.322(3)	0.9157(23)	1.1448(21)
Cl(2)	0.3246(17)	0.8651(15)	1.0204(14)
Cl(3)	0.1875(18)	0.8811(15)	1.1615(14)

[a] See footnote * of Table 1. [b] Population parameter 0.581. [c] Population parameter 0.419.

was a disubstituted triborate as determined from its ^{11}B n.m.r. spectra. Although it has not been isolated in the pure state, it is likely that a similar chlorination reaction had taken place to give $[B_3H_6Cl(NCO)]^-$.

When $[B_3H_7(NCS)]^-$ and $[B_3H_7(NCBH_3)]^-$ were treated with Hg_2Cl_2 in several solvents, they failed to yield disubstituted derivatives, although $[B_3H_7(NCO)]^-$ reacted to give a similar product mixture to that obtained from reactions with HCl.

(*ii*) *Substitution reactions.* In the substitution reactions of $[B_3H_6Cl_2]^-$ (1), one of the Cl substituents was replaced by a pseudo-halide, although the rate of substitution was slow compared with that of $[B_3H_7Cl]^-$. Thus, when $[B_3H_6Cl_2]^-$ was treated with Ag(NCS), the product was $[B_3H_6Cl(NCS)]^-$, but the reaction was less satisfactory as a preparative route than that of $[B_3H_7(NCS)]^-$ with HCl.

The reaction of $[B_3H_6Cl_2]^-$ with $[N(PPh_3)_2][BH_3(CN)]$ gave $[B_3H_6Cl(NCBH_3)]^-$ but the product was contaminated with $[B_3H_7(NCBH_3)]^-$. As such, it is another example of the dual chemical character of $[BH_3(CN)]^-$, in which the ion can act either as a donor ligand or as a hydride transfer reagent.[12] Although we have prepared $[B_3H_7(NCO)]^-$ from $[B_3H_7Cl]^-$, attempts to substitute $[B_3H_6Cl_2]^-$ with $[N(PPh_3)_2][NCO]$ were unsuccessful.

The reaction of $[B_3H_7Cl]^-$ with Ag(CN), which originally had been thought to produce $[B_3H_7(CN)]^-$, has recently been shown, by *X*-ray diffraction,[13] to yield the substituted silver

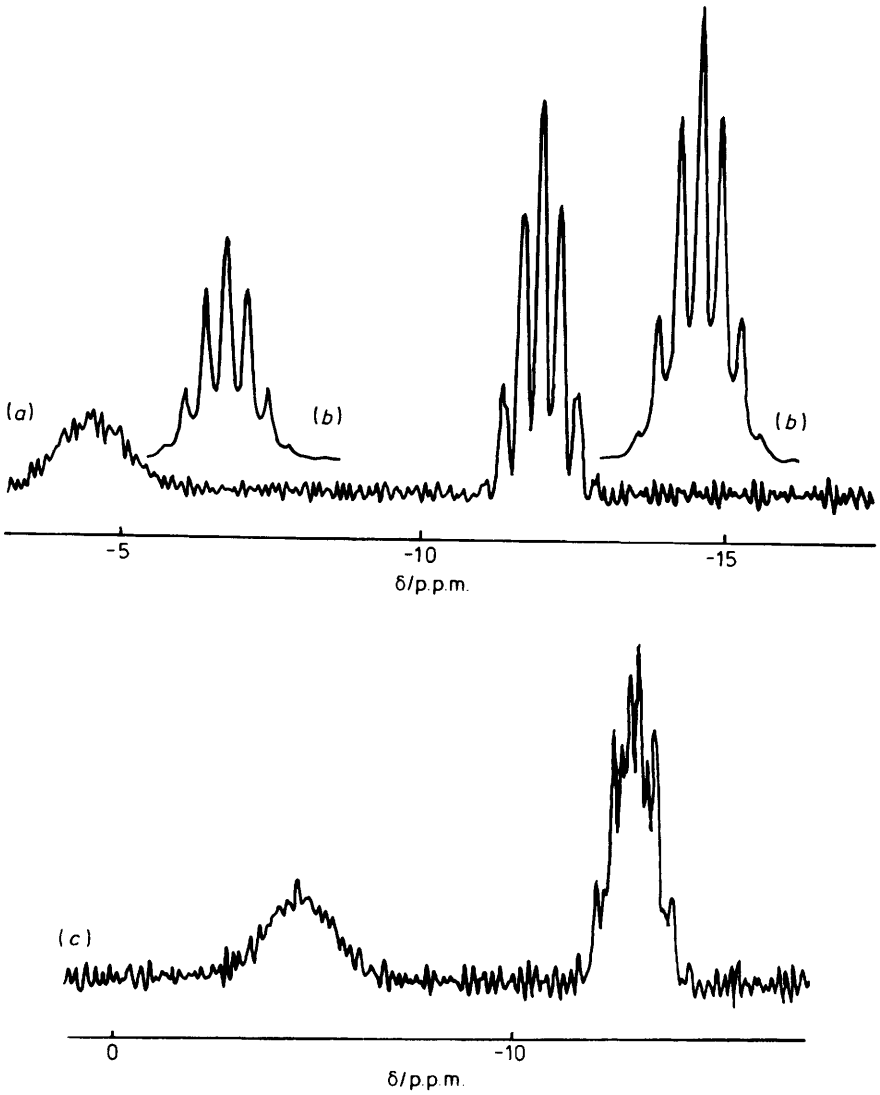

Figure 3. (*a*) 115.5-MHz ^{11}B N.m.r. spectrum (323 K) of $[B_3H_6Cl_2]^-$ in $CDCl_3$ (line narrowed), (*b*) simulated ^{11}B n.m.r. spectrum of $[B_3H_6Cl_2]^-$, (*c*) 80.4-MHz n.m.r. spectrum (298 K) of $[B_3H_6Cl_2]^-$ in CD_3CN (line narrowed)

anion $[Ag\{B_3H_7(NC)\}_2]^-$. The reaction of $[B_3H_6Cl_2]^-$ with Ag(CN) also yielded a cyanide-substituted triborane derivative, which had properties similar to $[Ag\{B_3H_7(NC)\}_2]^-$ and we believe this to be the anion $[Ag\{B_3H_6Cl(NC)\}_2]^-$; the proposed reaction is summarized in equation (iii). Solutions

$$2[B_3H_6Cl_2]^- + 3Ag(CN) \longrightarrow [Ag\{B_3H_6Cl(NC)\}_2]^- + CN^- + 2AgCl \quad \text{(iii)}$$

of $[Ag\{B_3H_7(NC)\}_2]^-$ and $[Ag\{B_3H_6Cl(NC)\}_2]^-$ decomposed on standing at room temperature, depositing silver.

We were unable to observe the substitution of the second Cl in substitution reactions. Thus when $[B_3H_6Cl(NCS)]^-$ was treated with Ag(NCS), the only species identified were unreacted starting materials along with some decomposition products.

The hydrolytic stability of the disubstituted anions has not been systematically studied, but whereas crystals of the $[B_3H_7Cl]^-$ ion hydrolysed within several hours on exposure to air, the crystalline $[N(PPh_3)_2]^+$ salts of $[B_3H_6Cl_2]^-$ and $[B_3H_6Cl(NCS)]^-$ deteriorated more slowly and survived several days exposure to air.

N.M.R. Spectra.—The ^{11}B n.m.r. spectra of $[B_3H_6Cl_2]^-$ in $CDCl_3$ and CD_3CN are shown in Figure 3. The two boron environments in the ratio of 2 : 1 each show coupling to six equivalent hydrogens, indicating fluxional behaviour.

The line-narrowed spectra failed to show well defined ^{11}B–^{11}B coupling in $CDCl_3$, whereas in CD_3CN some ^{11}B–^{11}B coupling was observed, although the spectra showed lines typical of partial quadrupolar relaxation. It has been shown previously that the observed line shape resulting from partial quadrupolar relaxation depends on the parameter α, which for ^{11}B, has the relationship [6,14] shown by equation (iv) (T_1 = relaxation time).

$$\alpha = \frac{5}{\pi T_1 J} \quad \text{(iv)}$$

The separation of 16 Hz of the apparent doublet from the substituted boron atoms in the ^{11}B-{^1H} spectrum of $[B_3H_6Cl_2]^-$ in CD_3CN must represent the maximum value for $J(^{11}B$–$^{11}B)$. Since the observed line shape corresponded to an α value near 5, the calculated relaxation time had a maximum value near 0.02 s. Since more extensive collapse of the multi-

Table 3. ^{11}B N.m.r. data [a] for substituted anions $[B_3H_6XX']^-$ at 115.5 MHz in $CDCl_3$

Substituents		δ(^{11}B)/p.p.m.				Weighted average shift
X	X′	B	B(X)	B(X′)	Other	
Cl [b]	Cl [b]	−4.3	−11.9(sp)			−9.4
Cl [c]	Cl [c]	−4.8	−11.8(sp)			−9.5
Cl [d]	CN [d]	−0.09	−3.41	−31.45		−11.65
Cl	NCS	−8.3	−4.2	−25.1		−12.5
Cl	NCO	−8.0	−6.9	−13.1		−9.3
Cl	$NCBH_3$	−2.09	−3.64	−30.5	−42.9(q)	−12.1
H	$NCBH_3$	−10.35		−34.94	−42.9(q)	

[a] q = Quartet, sp = septet. [b] At 303 K. [c] At 323 K. [d] In the complex $[Ag\{B_3H_6Cl(NC)\}_2]^-$.

Table 4. ^{11}B N.m.r. data * for substituted anions $[B_3H_6XX']^-$ at 80 MHz in $CDCl_3$

Substituents		δ(^{11}B)/p.p.m.				Weighted average shift
X	X′	B	B(X)	B(X′)	Other	
Cl	NCS	−8.85	−5.14	−25.9		−13.3
Cl	NCO	−8.8	−7.4	−14.0		−10.1
Cl	$NCBH_3$	−2.54	−4.27	−31.34	−43.6(q)	−12.7
Cl	$NCBH_2Cl$	−0.53		−31.34	−22.54(t)	−10.8
H	$NCBH_3$	−10.86		−35.48	−43.69(q)	
H	$NCBH_2Cl$	−9.60		−35.66	−22.54(t)	

* q = Quartet, t = triplet.

plet occurred in $CDCl_3$ with a line shape corresponding to an α value closer to 20, the relaxation time in this solvent was calculated to be nearer to 0.005 s. The observed coupling and the more extensive multiplet collapse in the lower polarity solvent are similar to effects observed earlier [6] for $[B_3H_7Cl]^-$. The explanation in terms of ion pairing presumably applies also to the disubstituted derivative.

The ^{11}B n.m.r. spectra in $CDCl_3$ of $[B_3H_6Cl(NCS)]^-$, $[Ag\{B_3H_6Cl(NC)\}_2]^-$, and $[B_3H_6Cl(NCBH_3)]^-$ each showed three unique boron chemical shifts. At ambient temperature, none of the compounds exhibited spectra in which either B–B or B–H couplings were resolved even with line narrowing. The details of the chemical shifts are presented in Tables 3 and 4 together with those of related compounds resulting from the preparative reactions.

The ^{11}B-{^1H} spectrum of $[B_3H_6Cl(NCS)]^-$ in CD_3CN, shown in Figure 4, exhibits some structure on line narrowing and is best interpreted on the basis of an ABC second-order (^{11}B–^{11}B–^{11}B) pattern, complicated by partial quadrupolar relaxation.

The assignments of the ^{11}B chemical shift to specific boron atoms are based on a comparison of the downfield shifts caused by the substituents in the monosubstituted derivatives with those in the unambiguous disubstituted derivatives. Additional support for the assignments came from the observation that the weighted average chemical shift of the boron atoms in the B_3 unit is shifted downfield from −29.8 p.p.m. in unsubstituted $[B_3H_8]^-$ to values in the range −17 to −21 p.p.m. in monosubstituted compounds $[B_3H_7X]^-$ (Table 5), and to values in the range −9 to −14 p.p.m. for the disubstituted derivatives $[B_3H_6XX']^-$.

Thermal Stability.—The crystalline solids $[N(PPh_3)_2][B_3H_6Cl_2]$ and $[N(PPh_3)_2][B_3H_6Cl(NCS)]$ were examined by d.s.c. and thermogravimetry. Neither compound showed any calorimetric changes below 100 °C. $[N(PPh_3)_2][B_3H_6Cl(NCS)]$ showed an endothermic change commencing at 105 °C with a peak at 118 °C, and two broad exothermic processes with peaks at 152 and 212 °C.

$[N(PPh_3)_2][B_3H_6Cl_2]$ exhibited a small exotherm near 127 °C, two other exotherms near 144 and 159 °C, and an endotherm near 227 °C. It is likely that the exothermic changes resulted from thermal changes within the borane anions whereas the first endotherm of $[B_3H_6Cl(NCS)]^-$ probably related to melting. Neither compound showed significant change in weight on heating to 280 °C.

Electrochemistry.—The electrochemical behaviour of the disubstituted anions was complex. Cyclic and a.c. voltammograms of $[B_3H_6Cl_2]^-$ and $[B_3H_6Cl(NCS)]^-$ at Pt in CH_3CN are shown in Figure 5. These indicate that the anions are more stable to oxidation than the monosubstituted derivatives, since irreversible oxidation waves were observed near 1.2 V. Coulometric oxidation of $[B_3H_6Cl_2]^-$ at the first oxidation wave indicated overall a one-electron oxidation process, but the products of oxidation have not yet been fully characterized. Similar one-electron oxidations were also observed in PhCN or 1,3-dioxolane, at either Pt or Cu anodes. When a Cu anode was used copper dissolution occurred, although the ^{11}B n.m.r. of the anodic products were similar for a given solvent to those obtained at Pt. Coulometric oxidation of $[B_3H_6Cl(NCS)]^-$ in CH_3CN at Pt involved 5—6 electrons, whereas in dioxolane only one electron was involved. At a copper anode, the ^{11}B n.m.r. spectra of the anodic products were similar to those at Pt when the compound was electrolyzed in dioxolane, but in CH_3CN mainly starting material was recovered. The products of all the electrochemical oxidations showed resonances near 21 p.p.m. (BF_3·OEt_2 reference).

Crystal Structures.—*trans*-$[N(PPh_3)_2][B_3H_6Cl_2$-1,2], (1).—Figure 6 presents a view of a single anion in a direction almost normal to the plane of the B_3 triangle, and demonstrates the atomic numbering scheme adopted. Table 6 contains interatomic distances and interbond angles.

Figure 4. 115.5-MHz ^{11}B-{^1H} N.m.r. spectrum of $[B_3H_6Cl(NCS)]^-$ in CD_3CN. B,B(X) resonance (line-narrowed)

Table 5. Chemical shift data [a] for ions $[B_3H_7X]^-$ at 80 MHz in $CDCl_3$

Substituent X	δ(^{11}B)/p.p.m. B_2	B(X)	Other	Weighted average shift
H	−29.8			−29.8
NCO	−21.3	−21.0		−21.2
NCS	−14.6	−33.9		−21.0
NCSe	−10.0	−33.1		−17.7
$NCBH_3$	−10.8	−35.5	−43.69(q)	−20.0
$NCBH_2Cl$	−9.6	−35.6	−22.54(t)	−18.3
$NCBPh_3$	−9.2	−34.7	−10.5	−17.7
CN [b]	−10.2	−36.8		−19.1
Cl	−16.9	−21.8		−18.5
Br	−12.2	−28.4		−17.8
F	−17.6	−15.4		−16.9

[a] q = Quartet, t = triplet. [b] In the complex $[Ag\{B_3H_7(NC)\}_2]^-$.

In $[B_3H_6Cl_2]^-$ the chlorine atoms are *trans*-1,2-substituents, with B–Cl (mean) 1.851(9) Å. This separation is longer than that typically found in chlorinated polyhedral boranes [15] or derivatives of borazine,[16] but is close to the value observed in BCl_3 adducts, *e.g.*, $PMe_3{\cdot}BCl_3$.[17] Simple calculation reveals that *cis*-1,2-disubstitution of the present molecule would result in an intramolecular Cl · · · Cl contact of *ca.* 3.34 Å, well below twice the van der Waals radius of Cl (3.6 Å).

The $[B_3H_6Cl_2]^-$ anion has two μ-H atoms, asymmetrically bridging the B(1)–B(3) and B(2)–B(3) connectivities. Overall, the ion has effective C_2 symmetry about the axis from B(3) to the midpoint of the B(1)–B(2) bond. The B_3 triangle is isosceles, B_{basal}–B_{basal} (mean) 1.804(13) Å, B_{basal}–H–B_{apical} (mean) 1.759(16) Å, Δ(B–B) = 0.045(21) Å. The only other authenticated dibridged B_3 species is $[B_3H_8]^-$; for this , too, relative lengthening of the non-bridged connectivity has been observed crystallographically [18] and successfully reproduced by geometry-optimised molecular orbital calculations.[19] In both studies [18,19] the dibridged structure of $[B_3H_8]^-$ has C_{2v} molecular symmetry, *i.e.* μ-H atoms lying in the plane of the B_3 triangle, and markedly asymmetric hydrogen bridges, *ca.* 0.3 Å shorter to B_{basal}. In $[B_3H_6Cl_2]^-$ similar asymmetry is clearly apparent [B–H bond length differences are 0.54 Å to H(13′) and 0.31 Å to H(23′)]; indeed we have reproduced the relative weakness of B_{apical}–μ-H that is implied from this lengthening by extended Hückel molecular orbital calculations

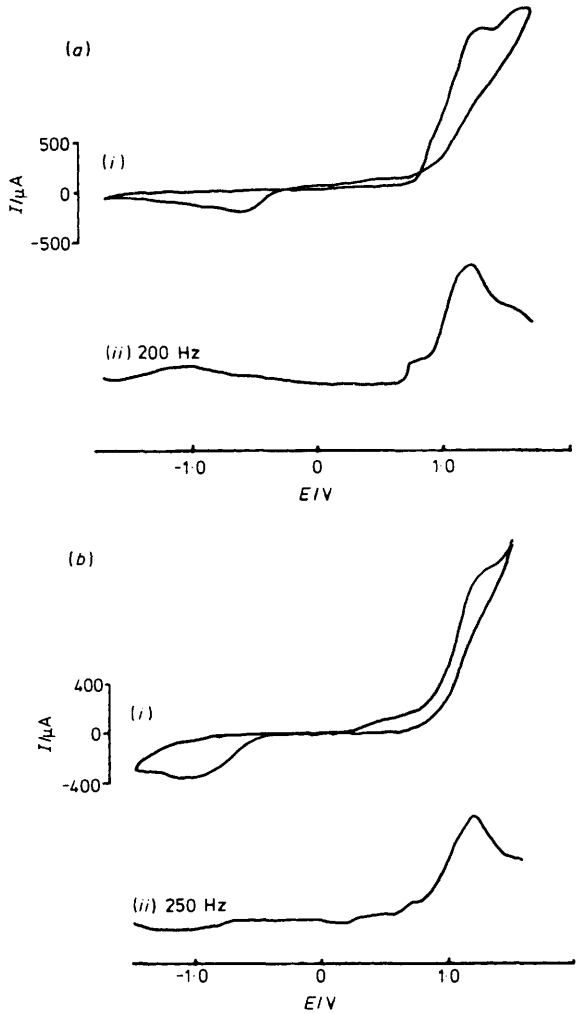

Figure 5. Cyclic (*i*) (0.1 mol dm^{-3} $[NBu^n_4][BF_4]$ in $CDCl_3$) and a.c. (*ii*) voltammograms of (*a*) $[B_3H_6Cl_2]^-$ and (*b*) $[B_3H_6Cl(NCS)]^-$ at Pt [0.5 V s^{-1} (*i*), 0.05 V s^{-1} (*ii*)]

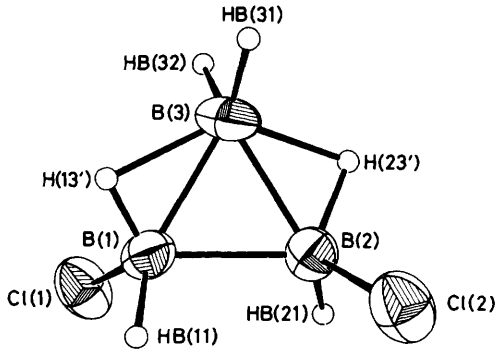

Figure 6. View of the $[B_3H_6Cl_2]^-$ anion normal to the plane of the B_3 triangle. Thermal ellipsoids are constructed at the 30% probability level, except for H atoms which have an artificial radius of 0.1 Å for clarity

Table 6. Molecular dimensions for $[B_3H_6Cl_2]^-$ (1); distances (Å) and angles (°)

P(1)–N(1)	1.583(5)	B(1)–H(13′)	1.00(8)
P(1)–C(11)	1.797(4)	B(1)–HB(11)	1.16(7)
P(1)–C(21)	1.794(4)	B(2)–B(3)	1.763(16)
P(1)–C(31)	1.785(4)	B(2)–Cl(2)	1.854(9)
P(2)–N(1)	1.576(5)	B(2)–HB(21)	1.07(7)
P(2)–C(41)	1.791(4)	B(2)–H(23′)	1.18(7)
P(2)–C(51)	1.793(4)	B(3)–HB(31)	1.05(8)
P(2)–C(61)	1.789(4)	B(3)–HB(32)	1.125(7)
B(1)–B(2)	1.804(13)	B(3)–H(23′)	1.47(8)
B(1)–B(3)	1.754(16)	B(3)–H(13′)	1.54(8)
B(1)–Cl(1)	1.848(9)		

N(1)–P(1)–C(11)	108.87(21)	B(1)–B(2)–HB(2)	101.0(40)
N(1)–P(1)–C(21)	109.36(21)	B(1)–B(2)–H(23′)	112.3(37)
N(1)–P(1)–C(31)	115.27(22)	B(3)–B(2)–Cl(2)	117.5(6)
C(11)–P(1)–C(21)	107.49(18)	B(3)–B(2)–HB(21)	131.3(40)
C(11)–P(1)–C(31)	106.99(19)	B(3)–B(2)–H(23′)	55.7(36)
C(21)–P(1)–C(31)	108.57(19)	Cl(2)–B(2)–HB(21)	111.3(40)
N(1)–P(2)–C(41)	111.61(21)	Cl(2)–B(2)–H(23′)	109.3(37)
N(1)–P(2)–C(51)	114.59(21)	HB(21)–B(2)–H(23′)	108.5(54)
N(1)–P(2)–C(61)	108.62(21)	B(1)–B(3)–B(2)	61.7(6)
C(41)–P(2)–C(51)	107.81(18)	B(1)–B(3)–HB(31)	139.1(43)
C(41)–P(2)–C(61)	107.28(18)	B(1)–B(3)–HB(32)	113.4(35)
C(51)–P(2)–C(61)	106.58(18)	B(1)–B(3)–H(13′)	34.7(29)
P(1)–N(1)–P(2)	138.9(3)	B(1)–B(3)–H(23′)	101.5(30)
B(2)–B(1)–B(3)	59.4(6)	B(2)–B(3)–HB(31)	124.6(43)
B(2)–B(1)–Cl(1)	115.0(6)	B(2)–B(3)–HB(32)	126.5(35)
B(2)–B(1)–H(13′)	116.7(44)	B(2)–B(3)–H(13′)	94.4(30)
B(2)–B(1)–HB(11)	96.3(36)	B(2)–B(3)–H(23′)	41.6(29)
B(3)–B(1)–Cl(1)	113.7(6)	HB(31)–B(3)–HB(32)	94.2(54)
B(3)–B(1)–H(13′)	60.6(44)	HB(31)–B(3)–H(13′)	111.7(51)
B(3)–B(1)–HB(11)	135.1(36)	HB(31)–B(3)–H(23′)	101.9(51)
Cl(1)–B(1)–H(13′)	105.7(44)	HB(32)–B(3)–H(13′)	104.2(44)
Cl(1)–B(1)–HB(11)	110.7(36)	HB(32)–B(3)–H(23′)	101.3(45)
H(13′)–B(1)–HB(11)	112.4(56)	H(13′)–B(3)–H(23′)	135.6(42)
B(1)–B(2)–B(3)	58.9(6)	B(2)–H(23′)–B(3)	82.8(44)
B(1)–B(2)–Cl(2)	114.1(6)		

(with parameters specified in Table 14 of SUP 23995) on an idealised, symmetrically bridged, model of *trans*-$[B_3H_6Cl_2$-1,2$]^-$, affording computed overlap populations of B_{apical}–μ-H 0.4309 and B_{basal}–μ-H 0.4611. Unlike the parent $[B_3H_8]^-$, however, the bridging H atoms in $[B_3H_6Cl_2]^-$ do not lie coplanar with the B_3 unit, but rather are displaced by *ca.* 0.31 Å to the opposite side of the plane from the adjacent Cl atom. Concomitantly, the apical $B(3)H_2$ fragment is twisted by *ca.* 14.8(3)° from the perpendicular bisector of B(1)–B(3)–B(2).

The $[N(PPh_3)_2]^+$ cation has effective C_2 symmetry about the in-plane bisector of the P–N–P angle, 138.9(3)°. The conformation about the P · · · P vector is *gauche*, having a 'mean torsion angle' [20] of 30.6(3)°. The planes of the phenyl rings which lie *anti* to the P–N–P angle are closely parallel [dihedral angle 8.2(3)°] and their centroids are separated by only 3.760(6) Å. Further details appear in Table 10 of SUP 23995. There are no close contacts between ion pairs. A packing diagram (Figure 8) is deposited in SUP 23995.

trans-$[N(PPh_3)_2][B_3H_6Cl(NCS)$-1,2$]\cdot CH_2Cl_2$, (2). This crystallographic study is only approximate, as discussed in the Experimental section. Table 7 lists bond lengths and angles determined at the termination of refinement, and Figure 7 displays the gross structure of the anion. No hydrogen atoms were located.

Generally, molecular dimensions have large e.s.d.s, particularly those within the anion, which preclude meaningful discussion. For example, the B(2)–B(3) distance obtained,

Table 7. Molecular dimensions for $[B_3H_6Cl(NCS)]^-\cdot CH_2Cl_2$ distances (Å) and angles (°)

P(1)–N(1)	1.581(11)	B(1)–N(2)	1.47(3)
P(1)–C(11)	1.782(10)	B(2)–B(3)	1.38(5)
P(1)–C(21)	1.781(9)	B(2)–Cl(1)	1.74(4)
P(1)–C(31)	1.781(12)	N(2)–C(1)	1.10(3)
P(2)–N(1)	1.583(11)	N(2)–C(2)	1.25(4)
P(2)–C(41)	1.783(8)	C(1)–S(1)	1.62(3)
P(2)–C(51)	1.793(9)	C(2)–S(2)	1.66(4)
P(2)–C(61)	1.790(9)	C(3)–Cl(2)	1.71(4)
B(1)–B(2)	1.82(5)	C(3)–Cl(3)	1.90(4)
B(1)–B(3)	1.74(5)		

N(1)–P(1)–C(11)	111.8(5)	B(2)–B(1)–B(3)	45.6(18)
N(1)–P(1)–C(21)	109.0(5)	B(2)–B(1)–N(2)	114.7(21)
N(1)–P(1)–C(31)	113.3(6)	B(3)–B(1)–N(2)	93.2(19)
C(11)–P(1)–C(21)	107.2(4)	B(1)–B(2)–B(3)	64.0(23)
C(11)–P(1)–C(31)	109.0(5)	B(1)–B(2)–Cl(1)	120.1(23)
C(21)–P(1)–C(31)	106.3(5)	B(3)–B(2)–Cl(1)	136.6(30)
N(1)–P(2)–C(41)	109.3(5)	B(1)–B(3)–B(2)	70.4(24)
N(1)–P(2)–C(51)	115.1(5)	B(1)–N(2)–C(1)	163.8(23)
N(1)–P(2)–C(61)	109.9(5)	B(1)–N(2)–C(2)	157.7(22)
C(41)–P(2)–C(51)	108.4(4)	C(1)–N(2)–C(2)	38.6(22)
C(41)–P(2)–C(61)	105.7(4)	N(2)–C(1)–S(1)	174.0(26)
C(51)–P(2)–C(61)	107.9(4)	N(2)–C(2)–S(2)	171.7(28)
P(1)–N(1)–P(2)	137.8(7)	Cl(2)–C(3)–Cl(3)	110.8(19)

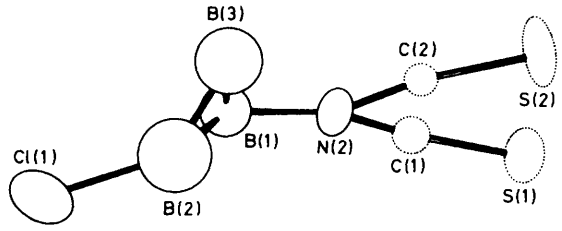

Figure 7. Perspective view of the $[B_3H_6Cl(NCS)]^-$ anion demonstrating the *trans*-1,2-disubstitution and disorder in the isothiocyanate function

1.38(5) Å, is almost certainly unrealistic. Nevertheless the *trans*-1,2-disubstitution pattern of $[B_3H_6Cl(NCS)]^-$ is clearly apparent, in spite of serious disorder of the NCS function.

The cation is again bent at N, 137.8(7)°, and has a *gauche* conformation, mean torsional angle 32.1(7)°. In addition to an intramolecular graphitic packing of ring C(31)—C(36) with ring C(51)—C(56), the phenyl group of C(61)—C(66) packs intermolecularly with its inversion related (through $\frac{1}{2},\frac{1}{2},1$) image (full details and a packing diagram are deposited as Tables 9—13 and Figure 9 in SUP 23995).

Acknowledgements

We thank the S.E.R.C. for a project grant (to J. H. M.) and use of the high-field n.m.r. service, and for funds (to A. J. W.) with which to purchase the diffractometer; the Thai Government for a research studentship (to M. A.); Borax Research Ltd. and the S.E.R.C. for a C.A.S.E. studentship (to S. J. A.); and the University of Edinburgh for a vacation studentship (to D. A. W.).

References

1 G. B. Jacobsen and J. H. Morris, *Inorg. Chim. Acta*, 1982, **59**, 207.

2 S. J. Andrews, A. J. Welch, G. B. Jacobsen, and J. H. Morris, *J. Chem. Soc., Chem. Commun.*, 1982, 749 and refs. therein; S. J. Andrews and A. J. Welch, *Inorg. Chim. Acta*, in the press.
3 G. E. Ryschkewitsch and V. A. Miller, *J. Am. Chem. Soc.*, 1975, **97**, 6258; *Inorg. Synth.*, 1974, **15**, 118.
4 W. H. Knoth, *Inorg. Chem.*, 1971, **10**, 598.
5 G. B. Jacobsen, J. H. Morris, and D. Reed, *J. Chem. Res.*, 1982, (*S*) 319, (*M*) 3601.
6 G. B. Jacobsen, J. H. Morris, and D. Reed, *J. Chem. Res.*, 1983, (*S*) 42, (*M*) 401.
7 G. M. Sheldrick, SHELX 76, University Chemical Laboratory, Cambridge, 1976.
8 'International Tables for *X*-Ray Crystallography,' Kynoch Press, Birmingham, 1974, vol. 4.
9 G. M. Sheldrick and P. Roberts, XANADU, University Chemical Laboratory, Cambridge, 1976.
10 J. M. Stewart, P. A. Machin, C. W. Dickinson, H. L. Ammon, H. Heck, and H. Flack, *X*-RAY 76, Technical Report TR-446, Computer Science Centre, University of Maryland, 1976.
11 C. K. Johnson, ORTEP-II, Report ORNL-5138, Oak Ridge National Laboratory, Tennessee, 1976.
12 G. B. Jacobsen, J. H. Morris, and D. Reed, *J. Chem. Soc., Dalton Trans.*, 1984, 415.
13 S. J. Andrews and A. J. Welch, unpublished work.
14 M. Suzuki and R. Kubo, *Mol. Phys.*, 1964, **7**, 201; M. Kubo, M. Watanabe, T. Totani, and M. Ohtsuru, *ibid.*, 1968, **14**, 367.
15 M. B. Hursthouse, J. Kane, and A. G. Massey, *Nature (London)*, 1970, **228**, 659.
16 W. Schwarz, D. Lux, and H. Hess, *Cryst. Struct. Commun.*, 1977, **6**, 431.
17 D. L. Black and R. C. Taylor, *Acta Crystallogr., Sect. B*, 1975, **31**, 1116.
18 C. R. Peters and C. E. Nordman, *J. Am. Chem. Soc.*, 1960, **82**, 5758.
19 M. L. McKee and W. N. Lipscomb, *Inorg. Chem.*, 1982, **21**, 2846.
20 C. Glidewell and D. C. Liles, *J. Organomet. Chem.*, 1981, **212**, 291.

Received 29*th December* 1983; *Paper* 3/2275